Available online at www.sciencedirect.com
SCIENCE DIRECT®
Aquatic Living Resources 16 (2003) 317–324
Aquatic Living Resources
www.elsevier.com/locate/aquliv

Vertical migration and dispersion of sprat (*Sprattus sprattus*) and herring (*Clupea harengus*) schools at dusk in the Baltic Sea

L.A. Fredrik Nilsson [a,*], Uffe Høgsbro Thygesen [b], Bo Lundgren [c], Bo Friis Nielsen [a], J. Rasmus Nielsen [b], Jan E. Beyer [b]

[a] *Informatics and Mathematical Modelling, Technical University of Denmark, Building 321, 2800 Kgs. Lyngby, Denmark*
[b] *Department for Marine Fisheries Research, Danish Institute for Fisheries Research, Charlottenlund Slot, 2920 Charlottenlund, Denmark*
[c] *Department for Marine Fisheries Research, Danish Institute for Fisheries Research, North Sea Centre, 9850 Hirtshals, Denmark*

Accepted 10 January 2003

Abstract

In populations of herring (*Clupea harengus*) or sprat (*Sprattus sprattus*), one typically observes a pattern of schools forming at dawn and dispersing at dusk, usually combined with vertical migration. This behaviour influences interactions with other species; hence a better understanding of the processes could contribute to deeper insight into ecosystem dynamics. This paper reports field measurements of the dispersal at dusk and examines two hypotheses through statistical modelling: that the vertical migration and the dissolution of schools is determined by decrease in light intensity, and that the dissolution of schools can be modelled by diffusion, i.e. active repulsion is not required. The field measurements were obtained during 3 days in March at one location in the Baltic Sea and included continuous hydroacoustical monitoring, trawl samples, and hydrographical CTD data. Echogram patterns were analysed using the school detection module in Echoview® and local light intensities were calculated using a model for surface illuminance. The data and the analysis support that schools migrate upwards during dusk, possibly trying to remain aggregated by keeping the local light intensities above a critical threshold, that schools initiate their dissolution when ambient light intensity drops below this critical threshold, and that fish subsequently swim in an uncorrelated random walk pattern.

Keywords: Random walk; Dispersion of schools; Light; Clupeids; Baltic

1. Introduction

When collecting hydroacoustic data in the Baltic, one commonly sees a fast change in the echogram structure at dawn and dusk. The day situation is often characterized by aggregations of clupeids close to the bottom, whereas there are disperse targets in the whole water column during the night. The pattern is similar to that of herring in the North Sea (Blaxter and Parrish, 1965; Blaxter, 1985), however, in the Baltic, a large proportion of the schools do not migrate vertically—they disperse in the initial phase of the transition close to the bottom. It is possible that most of the predator–prey interactions take place during the twilight period (Major, 1977; Clark and Levy, 1988); the swift changes seen on the echograms may be an indication of this. There are indications that both herring and sprat, and their main predator, cod, are feeding during dusk and dawn (Blaxter and Parrish, 1965; Adlerstein and Welleman, 2000) and consequently these periods could be very important for the population dynamics. This motivates an investigation of the spatial structure and how it changes during dusk and dawn.

The dominant species of fish in the Baltic Proper are sprat (*Sprattus sprattus*), herring (*Clupea harengus*), cod (*Gadus morhua*), and flounder (*Platichtys flesus*). Due to the relative scarcity of species, especially among schooling fishes, the Baltic is a well-suited study area for the transition between schooling and dispersed state in clupeids, since it is relatively easy to know what species one is studying and since the possible number of interactions between different species is few.

While there is some consistency as to where and when schools can be found, it remains much less clear why and how the transitions occur. One specific question is if school-

* Corresponding author.
E-mail address: afn@imm.dtu.dk (L.A.F. Nilsson).

doi:10.1016/S0990-7440(03)00039-1

ing fish actively spread out at dusk, or if schools simply diffuse as their members cease to maintain the structure. This article approaches this question by estimating the time constant of dissolution, assuming passive diffusion, and comparing with observed transition times. Another open question is how directly the dispersal is related to the decrease in light. We examine this issue by estimating the local light intensity at the position of observed schools.

2. Materials and methods

2.1. Data sampling and analysis

Data were collected during a survey with R/V Dana 12–14 March 2002. Two Simrad EY500 split-beam echosounders were continuously recording at 38 and 120 kHz, respectively. The hydroacoustical data were stored electronically. The transducers were hull mounted, and the echosounders were calibrated using standard procedures (Foote et al., 1986). Fish were collected using a TV3-trawl; it was used as a bottom trawl except for night hauls on March 14, when it was used for pelagic hauls. Hydrographical data were collected several times a day with a Seabird SBE911PLUS CTD equipped with a light sensor (Biospherical/Licor) that measures the photosynthetically active radiation (PAR). The collection of fish was performed during both day and night on approximately the same site.

The location at approximately 16° 20' E, 55° 45' N was chosen to be representative of the Bornholm basin with respect to species composition and depth range; the depth at this location was 55–65 m. The fish caught were minced and afterwards discarded into the sea at a dumping site 5 nmi away downstream in order to avoid disturbances to the study site. Steaming speed to and from the dumping site was 12 knots, otherwise the ship was operated at approximately 3 knots in order to make the acoustical data independent of whether the ship was trawling or not. The current direction was registered using an acoustic Doppler current profiler.

The hydroacoustical data were analysed using the Echoview software, version 2.20. The lower threshold for acceptance of volume backscattering values, S_v was set to –60 dB for echo-integration and school-detection procedures. The school detection parameters were set heuristically and the distances were based on GPS positions. The settings for the 38 kHz sounder were (120 kHz settings within parentheses): minimum school length 2 (1.20) m, minimum school height 2 (1.20) m, minimum connected height 1.5 (0.6) m, maximal vertical linking distance 3 (2) m, maximal horizontal linking distance 3 (7) m.

Both the EY500 and the Echoview software have algorithms for detecting the bottom. However, due to bad weather with high swell on March 14, the bottom identification did not perform well. Improved bottom values for pings were identified using a Matlab program searching for the maximum increase of echo level between samples near the expected depth obtained from nearby pings. Furthermore, to compensate for ship movements due to the swell, a C++ program was used to produce new raw data files in which data in relevant telegrams were shifted up or down in order to get bottom points aligned with a smoothed bottom line obtained by a moving average with Gaussian weights. The end result was a smoother bottom (see Fig. 1) and echogram patterns more comparable with the days with calm weather. We did not correct for bubbles under the ship. Regions that evidently were affected by this phenomenon were excluded from the analysis. Data from 0.5 m above bottom to 15 m below surface were included in the echo-integration and school-detection procedures. The upper limit was chosen since observed fish densities were very low above this depth and in order to exclude bubble noise on March 14.

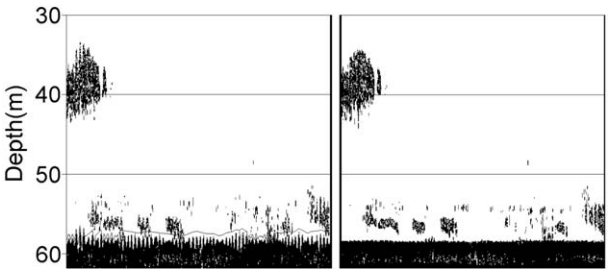

Fig. 1. Detail of echogram from March 14. Bottom is unsmoothed in the left panel, smoothed in the right.

The ship is equipped with a Licor PAR light sensor placed on the top of the ship, but its sensitivity was insufficient for measuring light intensities at dawn and dusk. Instead the light variations for twilight were estimated using a model by Janiczek and De Young (1987), which gives surface illuminance given time, date, geographical position and cloudiness. The cloudiness is given as four factors, corresponding to:

a Average clear sky, less than 70% of the sky covered by (scattered) clouds; the direct rays of the Sun or Moon are unobstructed relative to the location of interest.
b The Sun or Moon is easily visible but direct rays are obstructed by thin clouds.
c The direct rays of the Sun or Moon are obstructed by average clouds.
d Dark stratus clouds cover the entire sky (rare).

In the computer program, these conditions a–d correspond to dividing the calculated illuminance with a factor 1, 2, 3, 10, respectively. The model is quite crude (see Fig. 2). Since the sky was clear for most of the time, we have chosen to use the factor 1 or condition a.

The attenuation of light by water was estimated from the Seabird PAR data using a linear regression of the logarithm of light intensity on depth:

$$\ln I(z) = \ln I(0) - Kz \quad (1)$$

where $I(z)$, $I(0)$ are the light intensities at z and 0 m depth, respectively, and K is the attenuation coefficient. K was found to vary between 0.131 and 0.167 m^{-1}. We chose to proceed with a value of 0.16 m^{-1}, which is higher than the average value for the layer of interest, arguing that the rays of light during dusk come from a more or less horizontal light source.

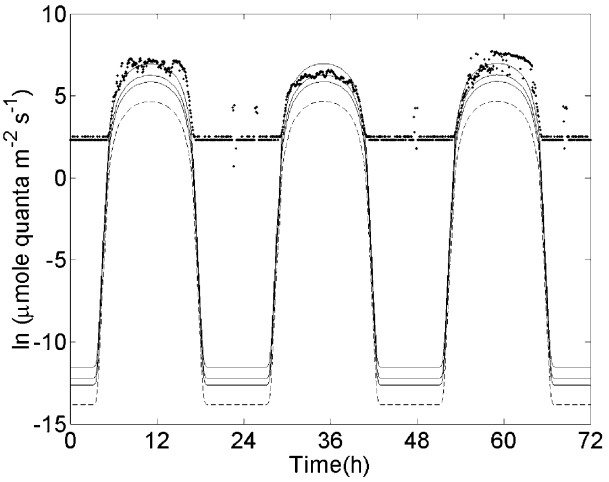

Fig. 2. Plot of logarithmic light intensities ln(µmol quanta s^{-1} m^{-2}). The dots are the measurements from the quantum light meter on R/V Dana. The black lines correspond to the four different cloud situations in the model for illumination (uppermost—clear, lowest—sky covered with stratus clouds). Horizontal scale is hours.

The attenuation is somewhat higher in the layer 0–10 m but we do not take this into account, since the relative effect of this is the same for all days and since only data below 15 m were analysed.

The surface illuminance from the model is given in lux, but the attenuation constant is based on PAR. We choose to use the factor 0.01953 µmol quanta s^{-1} m^{-2} lux^{-1} (Brock, 1981) to convert illuminance to surface PAR irradiance, assuming a standard daylight spectral distribution.

2.2. Migration process in relation to light levels

For every ping, the depth at which the local light intensities would correspond to 0.01, 0.1, 1 lux, respectively, were calculated using the daylight model and the attenuation coefficient. These light levels were chosen a priori since it has been reported that schooling ceased in this interval (Blaxter and Parrish, 1965; Iida and Mukai, 1996). The data were then displayed in the echograms as lines of equal irradiance. The schools followed the lines (see Fig. 3). With the Echoview school-detection module, we obtained the mean depth of a school and the time at which the school was recorded. In the same way as above, time was used to calculate the light intensity at the mean depth of the school. For data well within the transition period (17.25–18 UMT), we tested the model:

$$Y_{ij} = \alpha_i + \beta_i X_{ij} + \varepsilon_{ij} \quad (2)$$

where Y_{ij} is the natural logarithm of the light intensity at the depth of the centre of the jth school at the ith day, α_i, β_i are constants for day i, and X_{ij} is the depth of the jth school on day i, and ϵ_{ij} are independent and identically distributed normal variables with zero mean and variance σ^2. The log-transformation was necessary to meet the standard assumptions for linear regression.

2.3. Modelling the dissolution of schools by diffusion

This section constructs a model of the diffusion of schools and proposes three different time constants describing the duration of the process. With all three approaches, the number of fish in a typical school is Poisson distributed with mean $\bar{N}$ and the sizes of different schools are stochastically independent. At the starting point (dusk), all fish in the school are positioned at a single point in the plane. Then, instantly, all social forces are removed and each fish performs an independent random walk. The difference between the models is in how schools are placed at the starting point, and which criterion is used for the schools to have dissolved.

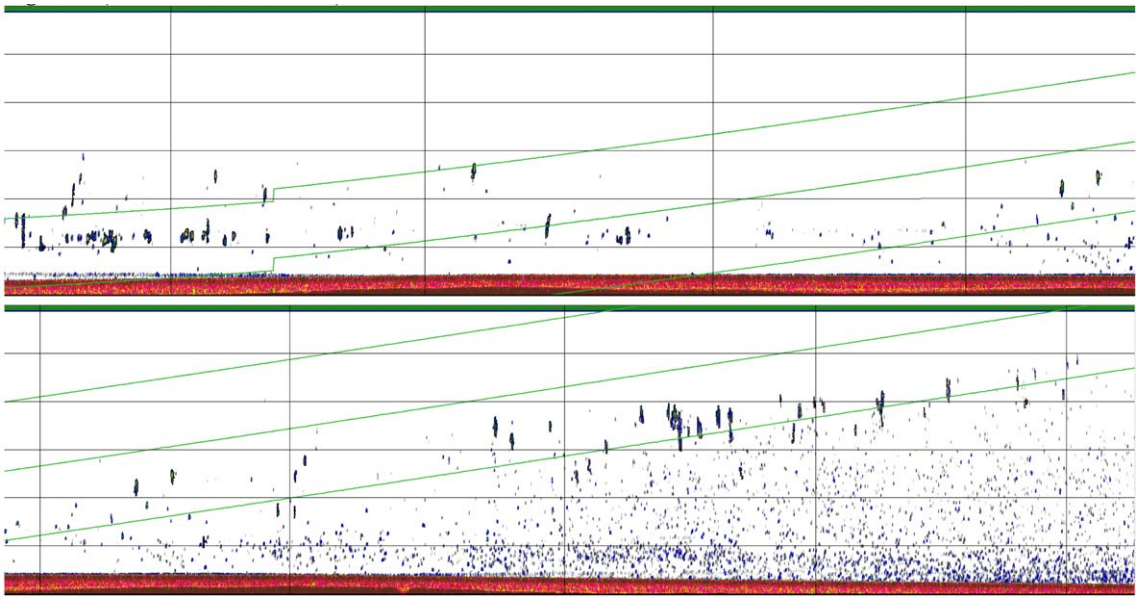

Fig. 3. The vertical migration of schools and dissolution at dusk on March 13. The three green parallel lines that rise from left to right are lines of equal light intensity. The step in the lines (left, top) is due to sunset. Distance between horizontal lines are 10 m and 0.5 nmi between vertical lines.

2.3.1. Dispersion from regularly spaced schools

At time $t = 0$ (dusk), a school is located at each node in a regular two-dimensional grid with grid length L. At times $t > 0$, each individual fish performs a random walk in two dimensions with intensity σ^2. The expected time until an individual fish has displaced itself a distance Δx from its starting point is (e.g. Berg, 1992).

$$\frac{\Delta x^2}{2\,\sigma^2} \tag{3}$$

If we insert $L/2$ for Δx, then we obtain roughly the time until the individual is halfway between two school centres; hence we cannot determine from which school the individual originated. Based on this argument, we would find that the time to dissolution of the schools is

$$\frac{1}{8}\frac{L^2}{\sigma^2} \tag{4}$$

Although this argument is somewhat sketchy, we shall see below that more elaborate modelling leads to similar answers.

2.3.2. Statistical detection of school structure

Using the same model as above, the individual fish constitute a Poisson point process (Stoyan et al., 1995) which is fully specified by its density $\rho(x,y,t)$. This density satisfies the partial differential equation (e.g. Berg, 1992):

$$\frac{\partial \rho(x, y, t)}{\partial t} = \frac{1}{2}\,\sigma^2\,\nabla^2\,\rho(x, y, t) \tag{5}$$

and can be expressed in terms of its Fourier series (Farlow, 1983):

$$\rho(x, y, t) = \sum_{k=-\infty}^{\infty}\sum_{l=-\infty}^{\infty} A_{kl}(t)\,\exp\left(i2\pi\,\frac{kx + ly}{L}\right) \tag{6}$$

Here, the coefficients $A_{kl}(t)$ are determined by the initial conditions, and are equal to:

$$A_{kl}(t) = \frac{\bar{N}}{L^2}\exp\left(-\frac{1}{2}\,\sigma^2\left(\frac{2\pi}{L}\right)^2(k^2 + l^2)\,t\right) \tag{7}$$

The shape of the solution is quickly dominated by the smallest non-zero eigenvalue, $-1/2\sigma^2\,(2\pi\,L)^2$, obtained with wave numbers $k^2 + l^2 = 1$.

At time T, we hypothetically sample two square regions, each of area $L^2/4$. One area, A, is centred around $(x,y) = (0,0)$ so that the initial position of the school is in the dead centre. The other, B, is centred at $(x,y) = (L/2,L/2)$ i.e. the point in space furthest away from the schools.

The number of fish found in region A, N_A, is then Poisson distributed with mean EN_A:

$$EN_A = \int_A \rho(T)\,\mathrm{d}x\,\mathrm{d}y = \sum_{k,l} A_{kl}(T)\,H_A(k, l) \tag{8}$$

where

$$H_A(k, l) = \int_A \exp\left(2\,\pi i\,\frac{kx + ly}{L}\right)\mathrm{d}x\,\mathrm{d}y = f(k)\,f(l) \tag{9}$$

and

$$f(k) = \int_{-L/4}^{L/4} \exp\left(2\,\pi i\,\frac{kx}{L}\right)\mathrm{d}x \tag{10}$$

We have that $f(k)$ is equal to $L/2$ when k is zero, otherwise it is $\frac{L}{2\,\pi i k}\left(\exp\left(\frac{\pi}{2}\,ik\right) - \exp\left(-\frac{\pi}{2}\,ik\right)\right)$. The latter expression is equal to 0 when k is even and non-zero. When k is odd, we have $f(k) = L/(\pi k)$, if $k = ..., -11, -7, -3, 1, 5, 9,...$, and $f(k) = -L/(\pi k)$, if $k = ..., -9, -5, -1, 3, 7, 11,....$ Now, focusing on the long-term behaviour, we consider only the lowest eigenvalue obtained with $k^2 + l^2 = 1$. Then

$$EN_A \approx \frac{L^2}{4}A_{0,0}(T) + \frac{L^2}{2\pi}\,(A_{0,1}(T) + A_{1,0}(T) + A_{0,-1}(T) + A_{-1,0}(T)) = \frac{\bar{N}}{4} + \frac{2\,\bar{N}}{\pi}\exp\left(-\frac{\sigma^2}{2}\left(\frac{2\pi}{L}\right)^2 T\right) \tag{11}$$

Correspondingly,

$$EN_B \approx \frac{L^2}{4}A_{0,0}(T) - \frac{L^2}{2\pi}\,(A_{0,1}(T) + A_{1,0}(T) + A_{0,-1}(T) + A_{-1,0}(T)) = \frac{\bar{N}}{4} - \frac{2\,\bar{N}}{\pi}\exp\left(-\frac{\sigma^2}{2}\left(\frac{2\pi}{L}\right)^2 T\right) \tag{12}$$

The criterion for the schools to have dissolved is that the $N_B > N_A$ with a certain probability $P = 1/2 - \alpha$. Approximating the Poisson distributions with Gaussians, we find

$$N_B - N_A \sim N\left(\frac{4\,\bar{N}}{\pi}\,e^{-\frac{\sigma^2}{2}\left(\frac{2\pi}{L}\right)^2 T}, \frac{\bar{N}}{2}\right) \tag{13}$$

And P is the probability of $N_B - N_A > 0$ which can then be approximated as

$$P = \frac{1}{2} - \alpha = \Phi\left(-\frac{4\,\sqrt{2\,\bar{N}}}{\pi}\,e^{-\frac{\sigma^2}{2}\left(\frac{2\pi}{L}\right)^2 T}\right) \tag{14}$$

where Φ is the standard Gaussian distribution function. Equivalently,

$$T = -\frac{L^2}{2\pi^2\,\sigma^2}\ln\left(\frac{\pi}{4\,\sqrt{2\,\bar{N}}}\,q\left(\frac{1}{2} + \alpha\right)\right) \tag{15}$$

where $q(1/2+\alpha)$ is the $(1/2+\alpha)$-quantile of the standard Gaussian distribution.

According to this expression for T, the natural time scale of the dissolution process is L^2/σ^2. In this time unit, we may plot T as a function of α for different values of N. This is done in Fig. 4. The most striking feature of the plot is the plateau, implying a fairly rapid transition from high levels of aggregation ($\alpha \approx 0.4$) to low levels of aggregation ($\alpha \approx 0.1$). This is comforting since it implies that the estimated transition time is not very sensitive to the exact choice of α, i.e. the critical level of aggregation. With this approach, the dependence on $\ln N$ is also quite natural; more fish in the school makes it easier to detect differences when they exist.

2.3.3. Dispersion from randomly placed schools

This model is a Poisson cluster model, using the terminology of stochastic geometry (Stoyan et al., 1995): schools are placed randomly in the plane according to a Poisson point process in 2D with intensity λ_s. To obtain the same density as in the previous model, we must have $\lambda_s L^2 = 1$. As before, school sizes are independent and identically Poisson distributed with mean $\bar{N}$, all fish within a school are co-located at

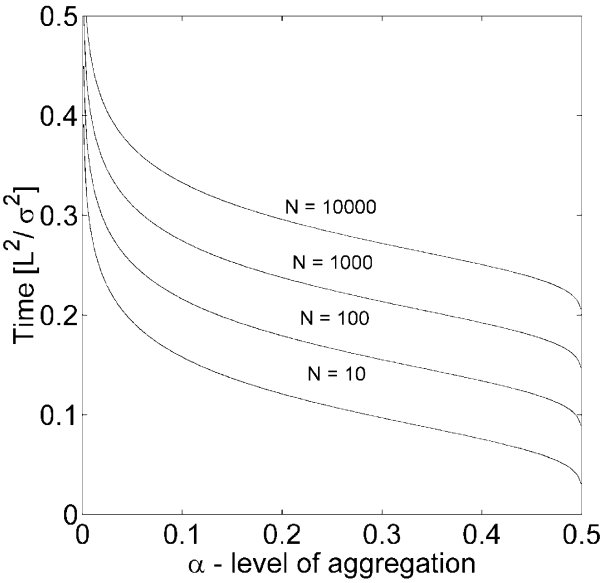

Fig. 4. Time against level of aggregation.

the school centre at time $t = 0$, and for time $t > 0$, each individual performs an independent Brownian motion with intensity σ^2.

At some later time t, the stochastic geometry becomes a Cox process, i.e. a conditional Poisson point process. To be specific, given the school centres, the density of the fish originating from the particular school is a Gauss bell, and the total density is the superposition of all these Gauss bells.

For a Poisson process, we can define the entropy as

$$I = -E \ln \rho(x, y) \tag{16}$$

i.e. minus the logarithmic density at a "typical point".

If only one school is present at position $(x,y) = (0,0)$, then at time t, individual fish will be distributed according to a Poisson process with density

$$\rho(x, y, t) = \frac{\bar{N}}{2\pi\sigma^2 t} e^{-\frac{1}{2}\frac{x^2+y^2}{\sigma^2 t}} \tag{17}$$

leading to an entropy

$$I = 1 + \ln 2\pi + \ln \sigma^2 t - \ln \bar{N} \tag{18}$$

where $\sigma^2 t$ is the variance in the 2D Gauss bell at time t. For low values of t, the schools do not interact and the same expression holds for the Poisson cluster model. As t grows, the entropy will gradually approach its limit in which the density is constant

$$\rho_\infty = \bar{N}\lambda_s \tag{19}$$

which leads to an entropy of $-\ln \bar{N}\lambda_s$. One way of assessing the time duration of the transition is to assume that the initial growth of entropy continues and then report the time where this entropy reaches the steady-state value. We find:

$$1 + \ln 2\pi + \ln \sigma^2 t - \ln \bar{N} = -\ln \lambda_s - \ln \bar{N} \tag{20}$$

or

$$t = \frac{1}{2\pi e \lambda_s \sigma^2} \tag{21}$$

2.4. Estimation of parameters

The inter-school distance was obtained with Echoview's school-detection module. Mean target strength was calculated from the TS relation (Foote, 1987) for clupeids and the length-distribution of caught herring and sprat. This was used to calculate the number of fish per school, assuming that schools could be described as vertical cylinders. The mean school area is (MacLennan and Simmonds, 1992) $\bar{A} = \frac{3\pi}{8}\bar{L}_0^2$, where $\bar{L}_0^2$ is the mean of squared length of schools.

3. Results

For the bottom and pelagic hauls, the catch consisted of more than 70% and 97% of clupeids, respectively (see Table 1). The size distributions were the same for bottom and pelagic hauls for sprat and herring (Fig. 5); the schools on the echograms are most likely sprat and herring.

The model for the relation between depth of school centres and local light conditions was significantly better at describing data than $Y_{ij} = \alpha_i$, i.e. that the logarithm of the light was independent of depth ($P < 0.002$). The model could be reduced to a model with a common slope; all β_i are equal (see Fig. 6). The model could not be reduced more, e.g. to zero slope or a common intercept. The residual plots did not indicate that the model was inappropriate. Since the error variance was high, the part of the variation that could be explained by the model was rather low, 0.22.

The distance between schools was found to be 70–200 m, the number of clupeids per school was 400–900, and the mean area was in the range 120–220 m^2.

Table 1
The weight and percentage of the species caught in the bottom hauls

Species	Common name	Fraction in bottom hauls	Fraction in pelagic hauls
Sprattus sprattus	Sprat	0.636	0.798
Clupea harengus	Herring	0.094	0.177
Platichtys flesus	Flounder	0.011	0
Gadus morhua	Cod	0.257	0.025
	Other species	0.002	≤ 0.001
Total weight (kg)		4387	914

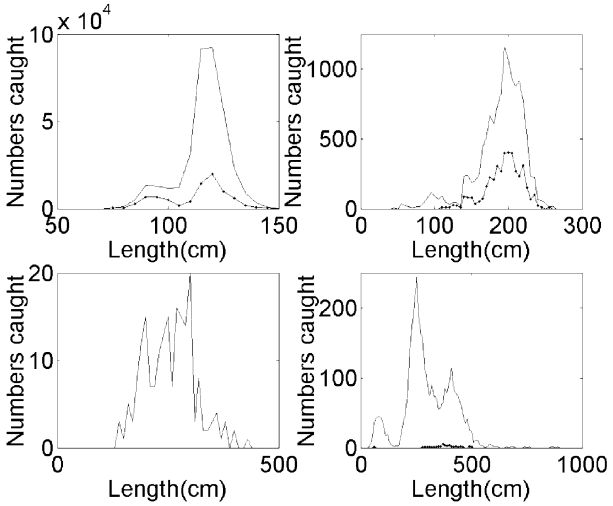

Fig. 5. The total numbers caught '—' in 20 hauls within a certain length-class of the dominant species sprat, herring, flounder and cod (top left, top right, bottom left, bottom right). The line joining dots '•—' shows fish caught with pelagic hauls (three hauls).

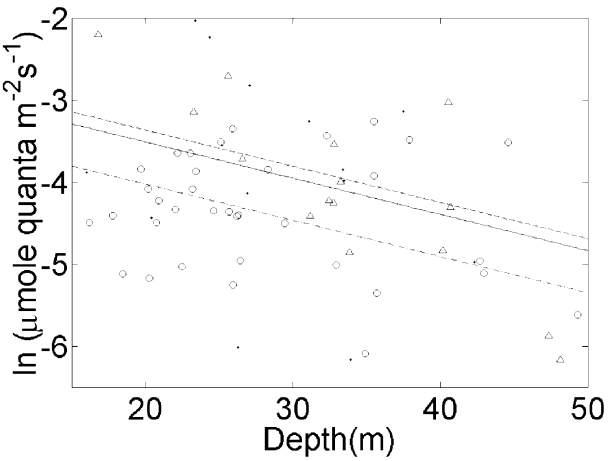

Fig. 6. Relationship between logarithm of light intensity at school centre and depth of school centre for 12–14 March 2002. Data from 12 March '•', 13 March 'o' and 14 March '△'. Fitted model for 12 March '—', 13 March '— —', and 14 March ' — —'.

Comparing the three suggested time constants of the transition, only the second time constant is based on statistical identification of school structures and hence grows with the number of fish in a typical school. Except for this difference, the time constants scale identically. Furthermore, for a school size between 10 and 10 000 fish, the estimated time constants are all of the same order of magnitude, i.e. between 0.05 and 0.3, measured in the time unit L^2/σ^2. In summary, a useful time constant of the dissolution process is about 0.1 L^2/σ^2 and after 0.3 L^2/σ^2, it is fair to say that the process has ceased.

To estimate L^2, we note that the average distance between schools during the daytime is 70–200 m. Since the width of the transect at the bottom is 7–8 m (7° beam width), this implies a school density of maximum one school per 490 m^2 and minimum one school per 1600 m^2.

To obtain a rough estimate of the diffusivity, we assume a swimming speed of one body length per second and a body length of 0.1 m, and a relaxation time (time between turns) of the swimming direction of 10 s. This yields $\sigma^2 = 0.1$ m^2 s^{-1} (Berg, 1992). The fraction $\frac{L^2}{\sigma^2}$ is then in the interval between 4900 and 16,000 s. Multiplying the former with 0.1 and the latter with 0.3, we obtain that the time for schools to dissolve is in the range between 8 and 80 min.

These models all assume that the fish in a school at time $t = 0$ are located at the same point. In reality, the size of a school is measurable compared to the typical distance between schools and thus the time constants should be seen as upper bounds.

4. Discussion

Some authors (Weston and Andrews, 1990; Fréon et al., 1996) have proposed that the dissolution, or expansion of schools may be due to a diffusion process, but not specified the underlying mechanism. In this paper, a simple model for the dissolution of schools is proposed, where the fish in a school disperse as uncorrelated random walkers. The models presented are based on few parameters and should be easy to use to compare with data in different regions. The estimated transition times are comparable to those observed, indicating that active dispersal is not required to explain the observed change in the pattern. Iida and Mukai (1995) obtained similar values for the dispersion of Kokkanee schools, 50 min; whereas Fréon et al. (1996) showed that, in Senegalese waters, the transition took several hours, but the expected values depend on the local conditions.

The results given by Orlowski (2001) suggest that there is a slower transition in the Baltic at dusk for herring and sprat that takes approximately 4 h; however that result is based on S_v per 30 min, not school identification. The slower transition could be explained with planktonic prey emerging from the bottom at dusk and that the fish dispersing close to the bottom are hungry enough to risk feeding and dispersing where the predation risk probably is very high since cod are close to the bottom. If the planktonic prey are rising slowly, then may be the dispersed fish close to the bottom follow their prey toward the surface, which would give rise to a slower transition phenomenon. This leads to an anisotropy that may give different time scales depending on whether the solution is determined in the horizontal or in the vertical plane. In a similar approach to Orlowski (2001), Giannoulaki et al. (1999) obtained a transition for sardines in the northern Aegean Sea that took several hours; it may be that the averaging done using S_v and the modelling of the vertical migration with relatively low order trigonometric polynomials give longer dispersion times.

Schools follow roughly the lines of equal light intensity, but with high variation. The fact that the schools rise faster than the lines of equal irradiance (i.e. $\beta < 0$) is difficult to explain. However, it should be noted that the differences

between the light intensities at the end points of the fitted lines are very small and perhaps the estimated slope β is an artefact of the methodology. In any case, the slope β being significantly different from 0 in the statistical sense should not overshadow the observation that schools appear to remain at similar light levels. It is encouraging that the models catch this feature despite the simplicity in their assumptions and the uncertainty on the parameters. The log-transformation of the light data makes biological sense, since the response of eyes is approximately logarithmic.

The fact that the model could not be reduced to a common intercept may be due to real differences between days or that the cloudiness factor in the model for the light illuminance is the same for the different days, while the light levels seem to differ between days (see Fig. 2).

The high variation in the results is partly due to few measurements. However, diurnal vertical migration is highly variable (e.g. Blaxter and Parrish, 1965; Appenzeller and Legget, 1995); it can vary over season, and is probably dependent on tides, the physiological status of the fish as well as predators (Blaxter and Parrish, 1965).

Appenzeller and Leggett (1995) showed that the modus and the upper 95 percentile of the biomass distribution of rainbow smelt (*Osmerus mordax*) closely follow the lines of constant local light intensities, whereas the lower 95 percentile did so to a lesser extent. The range of the vertical distribution was narrower during day than night. They also noted that the smelt formed dense schools during day, which dispersed during night. Based on our results, it is possible that the widening of the distribution is due to schools dissolving, and that the upper parts that followed light levels more closely were schools rising.

Future work should be aimed at describing the internal and external state of the schooling fish in the Baltic. Is the crepuscular period the time at which the clupeids are eating, being eaten, neither or both? Stomach data of both clupeids and cod with high temporal resolution could help to answer that question. If the dispersion pattern of a school were studied with sonar, this could possibly give the local swimming speeds of the fish, and a better overview of the process. In addition, it would be interesting to follow the individual fish during the dispersal of schools in laboratory tanks, such as was done by Blaxter and Parrish (1965). With modern tracking techniques, it should be able to obtain more information about the behaviour and motion of the individual fishes, and it might be important and informative to incorporate the predatory behaviour of cod in relation to clupeids, since predation is not a static risk but a dynamic process dependent on prey behaviour (Lima, 2002).

5. Conclusion

Schools of herring and sprat tend to follow lines of equal light intensity when they migrate towards the surface at dusk in the Baltic, whereas this is not the case for the dispersing fish. In contrast to other studies showing the phenomenon that migrating fish follow lines of equal light intensity, we have found that a large part of the schooling fish dispersed close to the bottom. This causes a widening of the depth distribution, which may be attributed to differences in hunger or some other internal factor. Three different measures for the time until schools are dispersed are presented, these agree quite well with the time-scales viewed on the echograms. The times depend on few parameters and should be useful in comparisons.

Acknowledgements

We wish to thank the crew of the R/V Dana for excellent work and the DIFRES personnel for processing the fish. The research was supported by the SLIP research school under the Danish Network for Fisheries and Aquaculture Research (www.fishnet.dk) financed by the Danish Ministry for Food, Agriculture and Fisheries and the Danish Agricultural and Veterinary Research Council. The work is part of a larger project ‘Development of improved models of fisheries impact on marine fish stocks and ecosystems’ also funded by the Danish Ministry for Food, Agriculture and Fisheries.

References

Adlerstein, S.A., Welleman, H.C., 2000. Diel variation of stomach contents of North Sea cod (*Gadus morhua*) during a 24-h fishing survey: an analysis using generalized additive models. Can. J. Fish. Aquat. Sci. 57, 2363–2367.

Appenzeller, A.R., Leggett, W.C., 1995. An evaluation of light-mediated vertical migration of fish based on hydroacoustic analysis of the diel vertical movement of rainbow smelt (*Osmerus mordax*). Can. J. Fish. Aquat. Sci. 52, 504–511.

Berg, H.C., 1992. Random Walks in Biology. 2d ed., Princeton Universtity Press, Princeton.

Blaxter, J.H.S., 1985. The herring: a successful species? Can. J. Fish. Aquat. Sci. 42 (Suppl. 1), 21–30.

Blaxter, J.H.S., Parrish, B.B., 1965. The importance of light in shoaling, avoidance of nets and vertical migration by herring. J. Cons. Perm. Int. Explor. Mer 30, 40–57.

Brock, T.D., 1981. Calculating solar radiation for ecological studies. Ecol. Model. 14, 1–19.

Clark, C.W., Levy, D.A., 1988. Diel vertical migrations by juvenile sockeye salmon and the antipredation window. Am. Nat. 131, 271–290.

Farlow, S.J., 1983. Partial Differential Equations for Scientists and Engineers. John Wiley & Sons, New York (Reprinted by Dover, 1992).

Foote, K.G., 1987. Fish target strengths for use in echointegrator surveys. J. Acoust. Soc. Am. 82, 981–987.

Foote, K.G., Aglen, A., Nakken, O., 1986. Measurements of fish target strength with a split-beam echosounder. J. Acoust. Soc. Am. 80, 612–621.

Fréon, P., Gerlotto, F., Soria, M., 1996. Diel variability of school structure with special reference to transition periods. ICES J. Mar. Sci. 53, 459–464.

Giannoulaki, M., Machias, A., Tsimenides, N., 1999. Ambient luminance and vertical migration of the sardine *Sardina pilchardus*. Mar. Ecol. Prog. Ser. 178, 29–38.

Iida, K., Mukai, T., 1995. Behavior of Kokanee *Oncorhynchus nerka* in Lake Kuttara observed by echo sounder. Fish. Sci. 61, 641–646.

Janiczek, P.M.J., De Young, J.A., 1987. Computer programs of Sun and Moon illuminance with contingent tables and diagram. Circ. US Nav. Obs. 171, 1–131.

Lima, S.L., 2002. Putting predators back into behavioural predator–prey interactions. Trends Ecol. Evol. 17, 70–71.

MacLennan, D.N., Simmonds, E.J., 1992. Fisheries Acoustics. Chapman and Hall, London.

Major, P.F., 1977. Predator–prey interactions in schooling fishes during periods of twilight: a study of the Silverside *Pranesus insularum* in Hawaii. Fish. Bull. 75 (2), 415–426.

Orlowski, A., 2001. Behavioural and physical effect on acoustic measurements of Baltic fish with a diel cycle. ICES J. Mar. Sci. 58, 1174–1183.

Stoyan, D., Kendall, W.S., Mecke, J., 1995. Stochastic Geometry and its Applications. 2d ed. Wiley, New York.

Weston, D.E., Andrews, H.W., 1990. Seasonal sonar observation of the diurnal schooling times of fish. J. Acoust. Soc. Am. 87, 673–680.